Available online at www.sciencedirect.com

ScienceDirect

Advances in Space Research 52 (2013) 1888–1901

ADVANCES IN SPACE RESEARCH (a COSPAR publication)

www.elsevier.com/locate/asr

Powered-descent trajectory optimization scheme for Mars landing ☆

Rongjie Liu [a], Shihua Li [a,*], Xisong Chen [a], Lei Guo [b]

[a] School of Automation, Southeast University, Nanjing 210096, China
[b] School of Automation Science and Electrical Engineering, Beihang University, Beijing 100191, China

Received 14 January 2013; received in revised form 3 August 2013; accepted 6 August 2013
Available online 16 August 2013

Abstract

This paper presents a trajectory optimization scheme for powered-descent phase of Mars landing with considerations of disturbance. Firstly, θ–D method is applied to design a suboptimal control law with descent model in the absence of disturbance. Secondly, disturbance is estimated by disturbance observer, and the disturbance estimation is as feedforward compensation. Then, semi-global stability analysis of the composite controller consisting of the nonlinear suboptimal controller and the disturbance feedforward compensation is proposed. Finally, to verify the effectiveness of proposed control scheme, an application including relevant simulations on a Mars landing mission is demonstrated.

Keywords: Trajectory optimization; Powered-descent; Mars landing; θ–D suboptimal method; Disturbance observer

1. Introduction

Planetary surface landing missions present an unique set of challenges about entry, descent, and landing (EDL). Take Mars landing mission as an example, the Martian atmosphere presents a unique and complex set of challenges to EDL (Gitelson et al., 2003; Braun and Manning, 2007; Korzun et al., 2010; Li et al., 2010), with only about 1% of the density of Earth's atmosphere. The atmosphere is too thin to provide appreciable deceleration yet sufficiently dense to generate substantial aerodynamic heating. However, the atmosphere is still thick enough to generate significant aerodynamic heating, requiring high performance heatshields on entry bodies. Moreover, it is difficult to predict the variability of the atmosphere with seasons, storms, and dust concentrations, which influences the process of EDL severely.

The EDL sequence mainly includes parachute descent phase and powered descent phase. Fig. 1 shows the sequence of events for the future representative Mars EDL baseline scenario (Steltzner et al., 2010), the lander enters a vertical descent phase before touchdown. So, the entire powered-descent process is required to be of a high degree of control precision, quality and stability. Otherwise, this would cause a failed landing attempt.

We mainly focus on the trajectory scenario to powered-descent of the Mars landing mission. For the simplify, 2-DOF model is considered in this paper. The nominal trajectory of powered-descent phase is pre-planned, then trajectory optimization can effectively reduce disturbance effects and then improve the control precision (Stryk and Bulibsch, 1992; Fahroo and Ross, 2000; Blackmore et al., 2010). In general, one of the trajectory design objectives is to minimize a defined performance index. There are a lot of optimal trajectory design articles about Mars landing (Sostaric, 2007; Topcu et al., 2007; Li and Peng, 2011; Park et al., 2011). In these papers, several numerical optimization algorithms are adopted to find approximate optimal solutions for the optimal control problems. However, it remains a challenge to precisely approximate the optimal solution with computations as less as possible.

☆ This work was supported by the National Basic Research Program of China (973 Program) (2012CB720003), the Program for New Century Excellent Talents in University (NCET-10-328).
* Corresponding author. Tel.: +86 025 83793785.
E-mail addresses: liurongjie09@126.com (R. Liu), lsh@seu.edu.cn (S. Li), chenxisong@263.net (X. Chen), lguo@buaa.edu.cn (L. Guo).

0273-1177/$36.00 © 2013 COSPAR. Published by Elsevier Ltd. All rights reserved.
http://dx.doi.org/10.1016/j.asr.2013.08.006

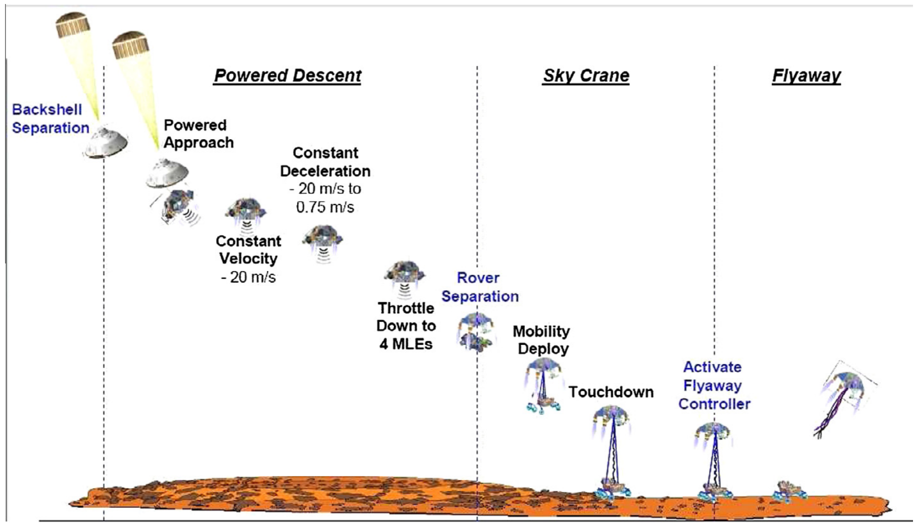

Fig. 1. MSL descent, and landing sequence of events.

Among existing numerous optimization methods, θ–D method (Xin and Balakrishnan, 2005) can avoid emerging large control action, and analytical solution can be obtained. It is a recursive algorithm resulting in a closed form optimal controller which does not need intensive online computations compared with the state dependent Riccati equation (SDRE) technique.

The main contribution of θ–D method is to find an approximate solution to the Hamilton–Jacobi–Bellman (HJB) equation. By introducing an intermediate variable θ, the optimal cost is expanded as a power series in terms of θ. The HJB equation is then reduced to a set of recursive algebraic Lyapunov equations, which are easier to solve in closed form because they are linear equations. In summary, the θ–D method essentially attempts to find a similar solution to the state dependent Riccati equation (SDRE) method, but avoids solving the Riccati equation online. The technique has already been applied in many fields, such as position and attitude control of spacecrafts (Xin et al., 2007) and longitudinal autopilot design of missiles (Xin and Balakrishnan, 2008). Moreover, θ–D method has been extended in some papers (Liu and Li, 2012, 2013) for dealing with optimal problems with various performance index forms.

When the disturbance exists, the disturbance can be estimated by disturbance observer. A nonlinear disturbance observer is developed for disturbances generated by an exogenous system, and global exponential stability is established under certain condition. The disturbance observer design can be separated from the feedback control design (Chen et al., 2000), this advantage can make optimization design perform robustly for systems with disturbances.

Specifically, for the disturbance observer (DOB) based optimal control approach, the original optimal control problem is divided into two subproblems (Chen, 2004). The first subproblem is the same as the control problem for a nonlinear nominal system and its objective is to stabilize the nonlinear plant and achieve performance specifications such as trajectory or regulation. The second subproblem is to attenuate disturbances. A nonlinear disturbance observer is designed to reject external disturbances and then to compensate for the influence of the disturbances. A composite nonlinear controller is constructed by combining feedback control with feedforward control , which globally exponentially stabilize the nonlinear system. In Chen et al. (2000) and Chen (2004), it is pointed out that the design of nominal controller is separated from design of the disturbance observer. In principle, it can be used to enhance the disturbance attenuation ability for any controller that cannot deal with disturbances or has poor disturbance attenuation ability.

In this paper, we focus on the design of trajectory optimization for power-descent phase of Mars landing. θ–D method is applied to design a suboptimal control law with nominal powered-decent model for the case of quadratic cost function. At the same time, disturbance is estimated by disturbance observer, and the disturbance estimation is employed as feedforward compensation. A nonlinear composite controller is skillfully constructed by suboptimal control and feedforward compensation. A rigorous proof is also given to show that semi-global stability of power-descent system of Mars landing with the composite controller consisting of the nonlinear suboptimal controller and the disturbance compensation. Finally, to verify the effectiveness of proposed control scheme, simulations on a Mars landing mission are demonstrated to examine the results of this solution.

The organization of the paper is as follows. Section 2 shows the model of powered-descent of Mars landing. In Section 3, controller design is presented, including the suboptimal control design and the disturbance observer design for estimating the disturbance. In Section 4, semi-global stability of power-descent system on Mars landing with the composite controller consisting of a nonlinear suboptimal control and a nonlinear disturbance observer is shown. Simulations relate to power-descent system of

Mars landing are demonstrated in Section 5 to examine the results of this solution. Our conclusions are given in Section 6.

2. Modelling of powered-descent of Mars landing

Consider an ideal point-mass module at the orbital of inertial frame (x, y) at t_0, which moves under the action of a constant propulsive force that makes a control angle $\beta(t)$ with the horizon. Obviously, the position and velocity vector of the vehicle will change due to the action of forces upon it. The problem is to determine the optimal trajectory strategy of this system for landing from a planet orbit by minimizing the quadratic cost function. For the simplify, 2-DOF model is considered in this paper. Based on Fig. 2, the lander dynamics powered-descent model of the Mars surface can be written as (Afshari et al., 2009; Izzo et al., 2011)

$$\begin{aligned}
&\dot{s} = v_s,\\
&\dot{v}_s = -\frac{T}{m}cos\beta + d_1,\\
&v\dot{h} = v_h,\\
&\dot{v}_h = \frac{T}{m}sin\beta - g + d_2,
\end{aligned} \tag{1}$$

where nomenclature as shown in Table 1, and mass m satisfies the mass equation $\dot{m} = -\frac{T}{I_{sp}g_0}$. The control laws are the thrust level and the thrust angle, T and β described, respectively. In fact, d_1 and d_2 are the acceleration disturbances in the actual system. e.g., aerodynamic drag and wind.

Let $a = \frac{T}{m}$, Eq. (1) can be rewritten as

$$\begin{aligned}
&\dot{s} = v_s,\\
&\dot{v}_s = -acos\beta + d_1,\\
&\dot{h} = v_h,\\
&\dot{v}_h = asin\beta - g + d_2.
\end{aligned} \tag{2}$$

These equations are suited to model only the descent and landing phases of a spacecraft at a preliminary stage, but they are nevertheless very useful to gain insight into

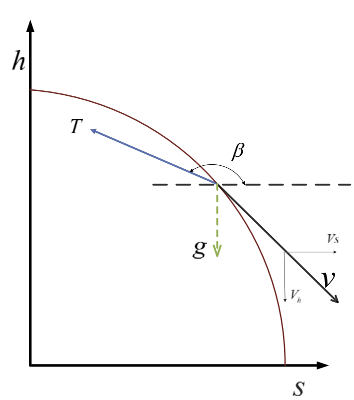

Fig. 2. Mars landing trajectory

Table 1
Nomenclature.

Cross range	s (m)
Height	h (m)
Cross velocity	v_s (m/s)
Vertical velocity	v_h (m/s)
State	$\mathbf{x}$
Thrust level	$T(N)$
Thrust angle	β (rad)
Control variables	$T(N),\ \beta$ (rad)
Landing mass	m (kg)
Mars gravity	g (m/s^2)
Earth gravity	g_0 (m/s^2)
Specific impulse	I_{sp} (s)
Time	t (s)
Disturbance	$d_1,\ d_2$ (m/s^2)

the structure of optimal control. Here we adopt a variable transformation. Let

$$s = x_1, \quad v_s = x_2, \quad h = x_3, \quad v_h = x_4,$$
$$u_1 = acos\beta, \quad u_2 = asin\beta - g.$$

Consequently, Eq. (2) reduces to

$$\begin{cases}
\dot{x}_1 = x_2,\\
\dot{x}_2 = -u_1 + d_1,\\
\dot{x}_3 = x_4,\\
\dot{x}_4 = u_2 + d_2,
\end{cases} \tag{3}$$

where $u_1^2 + (u_2 + g)^2 = a^2$.

For dynamic system (3), control law u_1 and u_2 will be designed. According to the coordinate change, thrust angle β in the original system can be derived as

$$\beta = \arccos\frac{u_1}{\sqrt{u_1^2 + (u_2 + g)^2}} \quad or$$
$$\beta = \arcsin\frac{u_2 + g}{\sqrt{u_1^2 + (u_2 + g)^2}}.$$

According to the mass equation $\dot{m} = -\frac{T}{I_{sp}g_0}$ and $a = \frac{T}{m}$. One obtains that the expression of thrust level T

$$T = a \cdot \exp\left(\ln m_0 - \frac{\int_0^t ads}{I_{sp}g_0}\right), \tag{4}$$

where m_0 is the initial value of landing mass.

Remark 1. In the next part, the closed-form expressions of a and β can be expressed by u_1 and u_2, which are solved by θ–D method. Since both u_1 and u_2 have the closed-form expressions, the closed-form expression of β can be obtained. Although control laws are the thrust level and the thrust angle, T and β described respectively, the expression of T cannot be given directly. However, by using the numerical solution and mass equation, we can obtain response curve of T.

With reference to the equations above, the optimal control problem is studied, and the quadratic cost function is considered here:

$$J = \frac{1}{2}\int_0^{\infty}[x^T Qx + u^T Ru]dt, \tag{5}$$

where $Q \in \mathbb{R}^{4\times4}$ is a semi-positive definite matrix and $R \in \mathbb{R}^{2\times2}$ is a positive definite matrix.

In next section, θ–D method will be applied to design a suboptimal control law for descent model in the absence of disturbance to minimize the quadratic cost function (5). Meanwhile, disturbance observer method will be used to estimate the disturbance, and the disturbance estimation will be employed as feedforward compensation. Then, a composite nonlinear controller is skillfully constructed by combining feedback control with feedforward control.

3. Control strategy design

In this paper, the procedure of controller design consists of two stages. Fig. 3 presents a block diagram of the control structure. In the first stage, the optimal controller is designed to achieve the performance function (5) without taking into disturbances account. θ–D method can be used to minimize the quadratic cost function. In the second stage, a nonlinear disturbance observer is designed, the disturbance estimation is employed as feedforward compensation. Then a composite nonlinear controller is skillfully constructed by combining feedback control with feedforward control . According to the results in (Chen et al., 2000; Chen, 2004), the design of optimal control is separated from design of disturbance observer.

3.1. Optimal control design

The optimal controller is designed to achieve the performance function (5) for nominal system. Then, we just consider the model relate to (3) without disturbance. Denote as

$$\dot{x} = Ax + Bu, \tag{6}$$

where

$$A = \begin{bmatrix} 0 & 1 & 0 & 0 \\ 0 & 0 & 0 & 0 \\ 0 & 0 & 0 & 1 \\ 0 & 0 & 0 & 0 \end{bmatrix}, \quad B = \begin{bmatrix} 0 & 0 \\ -1 & 0 \\ 0 & 0 \\ 0 & 1 \end{bmatrix}.$$

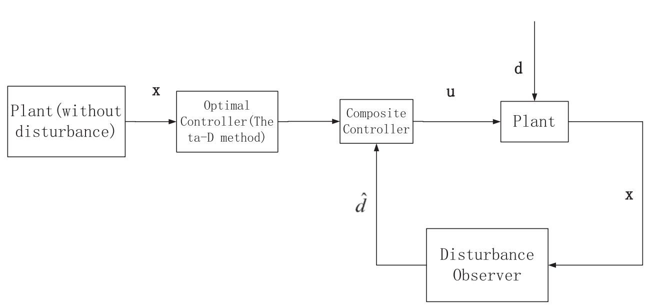

Fig. 3. Block diagram of the control structure.

To guarantee that there exists a unique solution near the origin for optimal control problem, some assumptions are listed as follows (Lukes, 1969).

Assumption 1. $x \in \Omega$ and Ω is a compact set including origin as an interior point, $u \in U$ and U is a compact set.

Assumption 2. System (6) is controllable and zero-state observable over the compact set Ω.

The Hamilton function for this optimal control problem is

$$H = \lambda^T[Ax + Bu] + \frac{1}{2}(x^T Qx + u^T Ru), \tag{7}$$

where $\lambda = \frac{\partial J^*}{\partial x}$ and $J^* = \min_u J$ with $J^* > 0$, $J^*(0) = 0$.

Taking derivative of the Hamilton function H with respect to u, yields

$$\frac{\partial H}{\partial u} = B^T\lambda + Ru = 0 \Rightarrow u = -R^{-1}B^T\lambda, \tag{8}$$

where λ is unknown and can be solved from the HJB equation, i.e.,

$$\lambda^T Ax - \frac{1}{2}\lambda^T BR^{-1}B^T\lambda + \frac{1}{2}x^T Qx = 0. \tag{9}$$

In Mars landing mission, the initial conditions of states, e.g., horizontal range and height, are usually large. As a result, it leads to large initial control magnitude. In order to overcome the problem of large control for large initial states, which is encountered by some other power series expansion based suboptimal control laws (Wernli and Cook, 1975), θ–D method is adopted to derive the approximate solution to the HJB equation.

Based on the results in Wernli and Cook (1975), in order to obtain a power series expansion of λ, let us add perturbation items $\sum_{i=1}^{\infty} D_i\theta^i$ to the cost function, which yields

$$\begin{aligned} J &= \frac{1}{2}\int_0^{\infty}[x^T Qx + u^T Ru]dt \\ &= \frac{1}{2}\int_0^{\infty}\left[x^T\left[Q_0 + \theta\frac{Q(x)}{\theta} + \sum_{i=1}^{\infty} D_i\theta^i\right]x + u^T Ru\right]dt. \end{aligned} \tag{10}$$

According to (9), the HJB equation with perturbations is

$$\lambda^T Ax - \frac{1}{2}\lambda^T BR^{-1}B^T\lambda + \frac{1}{2}x^T\left[Q_0 + \theta\frac{Q(x)}{\theta} + \sum_{i=1}^{\infty} D_i\theta^i\right]x = 0. \tag{11}$$

Assume that a power series expansion of λ is in terms of θ, i.e.,

$$\lambda = \sum_{i=0}^{\infty} T_i\theta^i x,$$

where $T_i, D_i,\ i = 1, \ldots, n$ are determined by the following equations

$$T_0 A + A^T T_0 - T_0 BR^{-1}B^T T_0 + Q_0 = 0, \tag{12}$$

$$T_1[A - BR^{-1}B^T T_0] + [A - BR^{-1}B^T T_0]^T T_1 = -\frac{Q(x)}{\theta} - D_1, \tag{13}$$

$$T_2[A - BR^{-1}B^T T_0] + [A - BR^{-1}B^T T_0]^T T_2 = T_1 BR^{-1}B^T T_1 - D_2, \tag{14}$$

$$\vdots$$

$$T_n[A - BR^{-1}B^T T_0] + [A - BR^{-1}B^T T_0]^T T_n = \sum_{j=1}^{n-1} T_j BR^{-1}B^T T_{n-j} - D_n, \tag{15}$$

$$D_1 = -\alpha_1 e^{-l_1 t}\frac{Q(x)}{\theta}, \tag{16}$$

$$D_2 = \alpha_2 e^{-l_2 t} T_1 BR^{-1}B^T T_1, \tag{17}$$

$$\vdots$$

$$D_n = \alpha_n e^{-l_n t}\sum_{j=1}^{n-1} T_j BR^{-1}B^T T_{n-j}, \tag{18}$$

where α_i and $l_i > 0,\ i = 1, \ldots, n$ are scalar adjustable design parameters satisfying $0 \leqslant 1 - \alpha_i e^{-l_i t} < 1,\ i = 1, \ldots, n$.

The expression for control can be obtained in terms of the power series as follows

$$u = -R^{-1}\left[B^T \sum_{i=0}^{\infty} T_i \theta^i\right] x. \tag{19}$$

By substituting the expressions of $D_i,\ i = 1, \ldots, n$ (see Eqs. (16)–(18)) into (13)–(15), it can be easily found that, $\frac{1}{\theta^i}$ appears linearly in Eqs. (13)–(15). Since $T_i,\ i = 1, \ldots, n$ multiplies θ^i in the control, θ can be dropped off.

Remark 2. We denote $\hat{T}_0 = T_0,\ \hat{T}_i = \theta^i T_i,\ \epsilon_i = 1 - \alpha_i e^{-l_i t}$, $i = 1, \ldots, n$. In next section, we will discuss the properties of $\sum_{i=0}^{\infty} \hat{T}_i$ instead of $\sum_{i=0}^{\infty} T_i \theta^i$ for the purpose of convenience of stability analysis.

Remark 3. In practical applications, it is unnecessary to derive all T_i terms. Usually, in order to simplify calculating, we only calculate first several T_i terms, and it is reasonable to use the summation of first several T_i terms to approximate the series $\sum_{i=0}^{\infty} T_i$.

3.2. Disturbance observer design

Disturbances can be reasonably estimated if the disturbance observer dynamics are faster than that of the closed-loop system. The same argument for the state observer based control methods is valid. For the sake of simplicity, one assumption on the disturbances is presented below. Similar assumptions can be found in Yang et al. (2011) and Li et al. (2013).

Assumption 3. Suppose that the disturbances and their derivatives are bounded and the derivatives satisfy $\lim_{t\to\infty} \|\dot{d}(t)\| = 0$.

Remark 4. The Assumption 3 is common in the field of disturbance estimation and rejection (see Chen et al., 2000; Li et al., 2012; Yang et al., 2013 etc). In practice, even though the derivative of disturbances does not converge to zero (i.e. $\dot{d} \nrightarrow 0$) but being bounded, the proposed disturbance observer can still effectively estimate the disturbance, of which the bound can be adjusted by means of appropriately designing the observer gain. The practical stability of the observer system is still satisfied.

For system (3), the following observer is designed to estimate the disturbances $d = [d_1, d_2]^T$ (Yang et al., 2011).

$$\begin{aligned} \dot{z} &= -LB_d(z + Lx) - L(Ax + Bu), \\ \hat{d} &= z + Lx, \end{aligned} \tag{20}$$

where $x = [x_1, x_2, x_3, x_4]^T,\ u = [u_1, u_2]^T, B_d$ is the coefficient matrix of disturbances d in (3), z is an auxiliary vector and L is the observer gain matrix to be designed.

Remark 5. According to the results in Li et al. (2013), it is known that the estimates $\hat{d}$ of disturbance observer (20) asymptotically track the disturbances d if the observer gain matrix L is chosen such that $-LB_d$ is a Hurwitz matrix.

3.3. Composite nonlinear controller

Thus, combining Eq. (19) with Eq. (20), the control law for model (3) is derived as

$$u = -R^{-1}\left[B^T \sum_{i=0}^{\infty} T_i \theta^i\right] x - C_d \hat{d}, \tag{21}$$

where matrix C_d satisfies $BC_d = B_d$. As a result, the original control laws in model (1) can be obtained,

$$\beta = \arccos\frac{u_1}{\sqrt{u_1^2 + (u_2 + g)^2}} \quad or \quad \beta = \arcsin\frac{u_2 + g}{\sqrt{u_1^2 + (u_2 + g)^2}}, \tag{22}$$

where u_1 and u_2 are the components of control law u.

4. Stability analysis

After the nonlinear disturbance observer is designed as in (20), a composite nonlinear controller is constructed by combining feedback control with feedforward control. In this section we will investigate the stability of closed-loop system under the composite controller. The main result of this section is stated in Theorem 1. Before we state this Theorem, Lemmas 1–4 are given first, which will be applied in the proof of Theorem 1.

Lemma 1 Xin and Balakrishnan (2005). *If the following conditions are satisfied*:

(i) Q_0 *is semi-positive definite*,
(ii) $\lambda_{max}[(A - BR^{-1}B^T\hat{T}_0) + (A - BR^{-1}B^T\hat{T}_0)^T] < 0$, *where* λ_{max} *denotes the largest eigenvalue, the series* $\sum_{i=0}^{\infty}\hat{T}_i$

produced by the algorithm is pointwise convergent and positive definite.

Lemma 2 Khalil (2002). *Let $V : [0,\infty) \times R^n \to R$ be a continuously differentiable function such that*

$$\alpha_1(\|x\|) \leqslant V(t,x) \leqslant \alpha_2(\|x\|), \tag{23}$$

$$\frac{\partial V}{\partial t} + \frac{\partial V}{\partial x} f(t,x,u) \leqslant -W_3(x), \forall \|x\| \geqslant \rho(\|u\|) > 0, \tag{24}$$

$\forall (t,x,u) \in [0,\infty) \times R^n \times R^m$, where α_1, α_2 are class κ function, and $W_3(x)$ is a continuous positive definite function on R^n. Then, the system

$$\dot{x} = f(t,x,u), \quad x \in R^n, \quad u \in R^m \tag{25}$$

is input-to-state stable (ISS) with $\gamma = \alpha_1^{-1} \circ \alpha_2 \circ \rho$.

Lemma 3 Khalil (2002). *Consider a nonlinear system $\dot{x} = F(x,\omega)$ which is ISS. If the input satisfies $\lim_{t\to\infty}\omega(t) = 0$, then the state $\lim_{t\to\infty}x(t) = 0$.*

Lemma 4 Khalil (2002). *Consider the following cascade system*

$$\dot{x}_1 = f_1(t,x_1,x_2), \tag{26}$$

$$\dot{x}_2 = f_2(t,x_2). \tag{27}$$

The cascade system (26) and (27) is globally uniformly asymptotically stable if the following conditions are satisfied.

(i) *System $\dot{x}_1 = f_1(t,x_1,0)$ is globally uniformly asymptotically stable.*
(ii) *System (26) is input-to-state stable w.r.t.x_2.*
(iii) *System (27) is globally uniformly asymptotically stable.*

Remark 6. According to the proof of Lemma 4 in Khalil (2002), it can be similarly derived that, the cascade system (26) and (27) is semi-globally uniformly asymptotically stable if systems $\dot{x}_1 = f_1(t,x_1,0)$ and (27) are both semi-globally uniformly asymptotically stable and condition (ii) is satisfied.

Theorem 1. *If Assumptions 1–3 and the two conditions in Lemma 1 are satisfied, D_i, $i = 1,\ldots,n$ are chosen such that $Q + \sum_{i=1}^{\infty} D_i\theta^i$ is semi-positive definite and the observer gain matrix L is chosen such that $-LB_d$ is a Hurwitz matrix, then control law (21) semi-globally asymptotically stabilizes system (3).*

The proof of Theorem 1 is omitted. The details of proof is in Appendices.

5. Simulation results

The parameters in the controller are set as follows: the parameters $Q = 0.01 * \mathbf{I}_4$, $R = 50 * \mathbf{I}_2$, the observer gain matrix L is designed as

$$L = \begin{bmatrix} 0 & 10 & 0 & 0 \\ 0 & 0 & 0 & 20 \end{bmatrix}$$

and $\epsilon_1 = 1$, $\epsilon_2 = 1$, $l_1 = 100$, $l_2 = 500$. The parameters in Mars landing model (1) are set as below: the initial states $(x_1(0), x_2(0), x_3(0), x_4(0)) = (0\ \text{m}, 65\ \text{m/s}, 1600\ \text{m}, -35\ \text{m/s})$; the terminal states $(x_1(t_f), x_2(t_f), x_3(t_f), x_4(t_f)) = (1000\ \text{m}, 0\ \text{m/s}, 0\ \text{m}, 0\ \text{m/s})$; $m_0 = 2000$ kg; $g = 3.7114\ \text{m/s}^2$; $g_0 = 9.8\ \text{m/s}^2$; $I_{sp} = 114$ s.

Three cases are taken into account here. In Case 1, we consider the model (1) with $d_1 = 0\ \text{m/s}^2$, $d_2 = 0\ \text{m/s}^2$. The simulation results are presented in Figs. 4–6. In Case 2, the disturbances d_1, d_2 are set as: $d_1 = 10\ \text{m/s}^2$ for $20 \leqslant t \leqslant 22$ and $d_2 = 10\ \text{m/s}^2$ for $28 \leqslant t \leqslant 30$ respectively. In Case 3, the disturbances d_1, d_2 are set as: $d_1 = 5 * \sin(0.5\pi * t)\ \text{m/s}^2$ for $12 \leqslant t \leqslant 16$ and $d_2 = 5 * \cos(0.5\pi * t)\ \text{m/s}^2$ for $16 \leqslant t \leqslant 20$ respectively.

Remark 7. In fact, the disturbances d_1, d_2 in the simulation study can actually represent a large range of disturbances. The step disturbance can be seen as the sudden unknown input to the system in a short time, while the sinusoidal one actually can represent the periodical disturbance.

The simulation results are shown from Figs. 4–12. It can be found that the Mars landing model has good robustness and ability of anti-disturbance under our proposed controller.

In practical applications, it is unnecessary to derive all T_i terms. In order to simplify calculating, we only calculate first several T_i terms, i.e., T_0, T_1, T_2 and T_3. In Case 1, since the disturbances in model (1) are not taken into account, the results based on θ–D method are performed in Figs. 4 and 5. In Cases 2 and 3, the proposed control method is applied on the Mars landing model with disturbances. In Figs. 4, 8 and 11, the solid lines represent the response curves of x_1 and x_3 in two cases respectively. It can be found that, although the disturbances exist in Cases 2 and 3, the states reach the desired position after about 30 s, the same as that in Case 1.

In Figs. 8 and 11, the solid lines represent the response curves of disturbances while the dotted lines represent the response curves of the disturbance estimations in Cases 2 and 3. It is observed from these two figures that the disturbance observer with the above designed parameters has achieved quite fine disturbance estimation performances.

In Figs. 5, 9 and 12, the solid lines represent the response curves of the thrust level T and the thrust angle β in Cases 1–3 respectively. In the simulation results, the maximum thrust is about 20000 N. There is a constraint on the angle rate, i.e., $|d\beta/dt| \leqslant 0.12$. Here we use the soft constraint method to handle this issue. The details of implementing the soft constraint method can be found in de Oliveira and Biegler (1994), Fletcher (1987) and Fruhwirth and Abdennadher (2003). The related plot of the angular rate is presented in Fig. 6. According to the results in Afshari

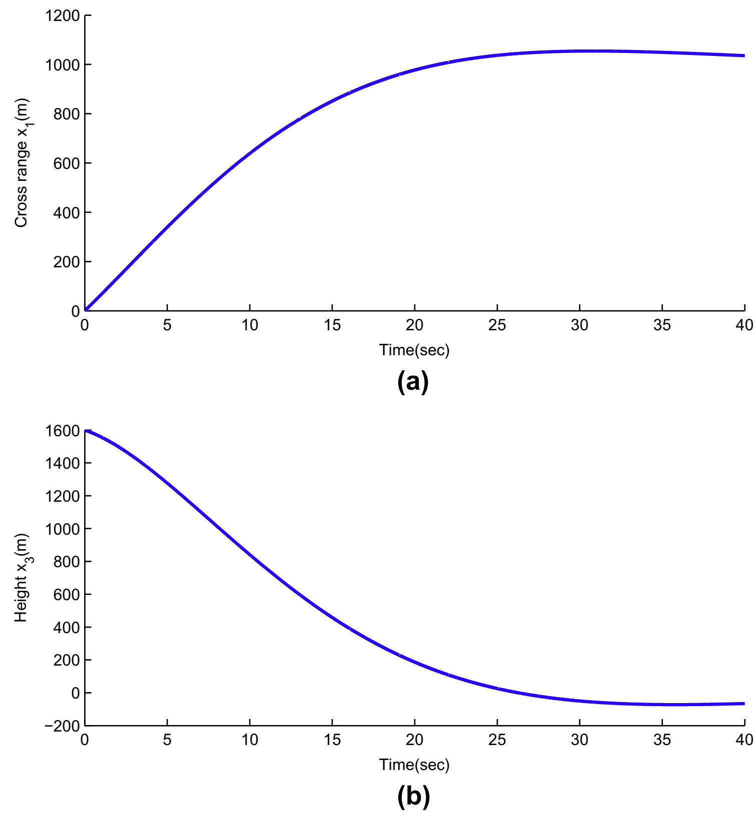

Fig. 4. Response curves of cross range x_1 and height x_3 of Mars landing model in Case 1. (a) x_1, (b) x_3.

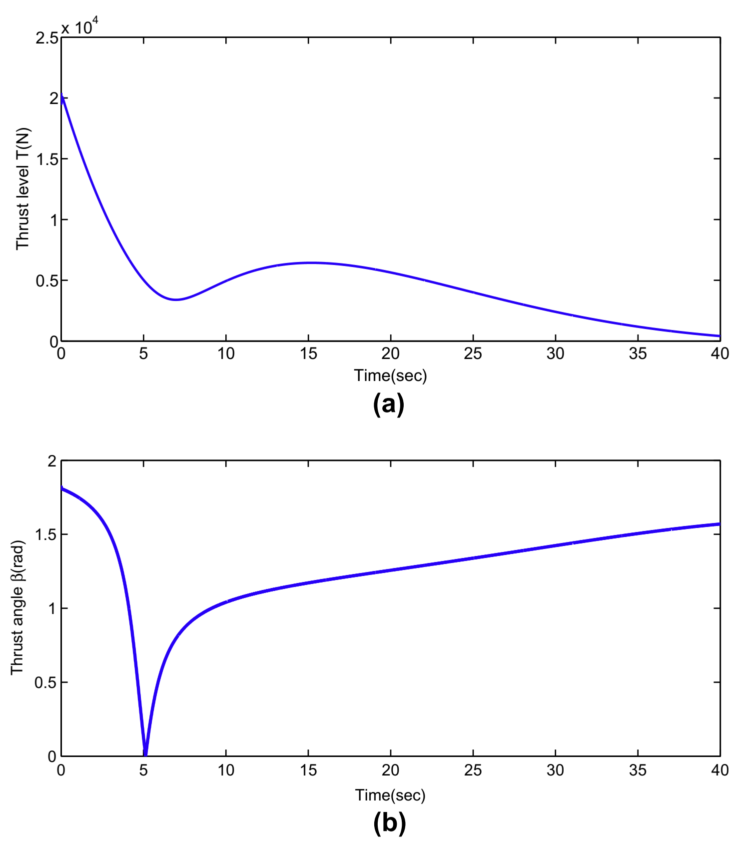

Fig. 5. Response curves of the thrust level and thrust angle of Mars landing model in Case 1. (a) T, (b) β.

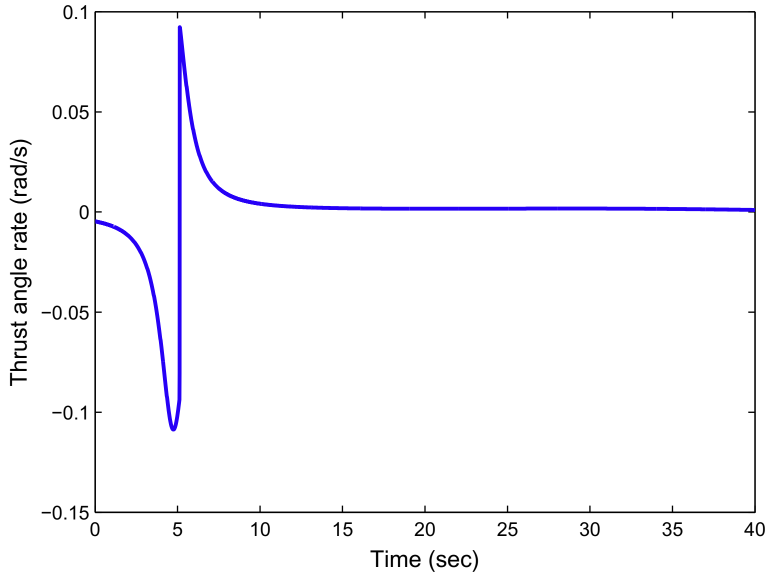

Fig. 6. Response curve of the thrust angle rate of Mars landing model in Case 1.

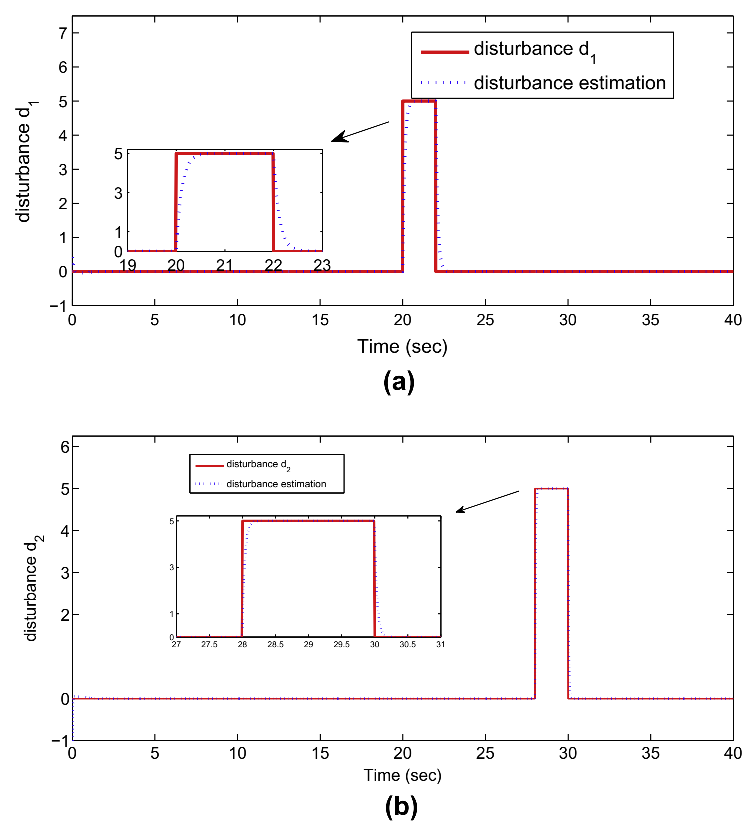

Fig. 7. Response curves of disturbance estimations of Mars landing model in Case 2. (a) $\hat{d}_1$, (b) $\hat{d}_2$.

et al. (2009, 2011), the soft constraint of the angle rate in this paper is reasonable.

For Case 3, we compare our proposed method with the ordinary linear controller,

$$u_1 = x_1 + 2x_2; \quad u_2 = -x_3 - 3x_4. \tag{28}$$

It can be easily derived that the linear controller (28) globally asymptotically stabilizes the system (3), and the

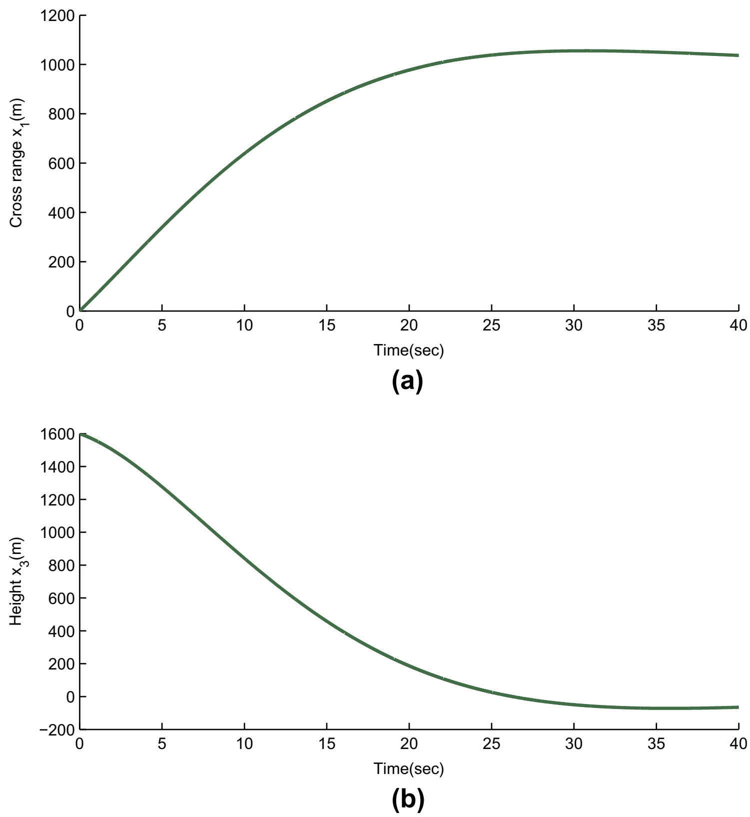

Fig. 8. Response curves of cross range x_1 and height x_3 of Mars landing model in Case 2. (a) x_1, (b) x_3.

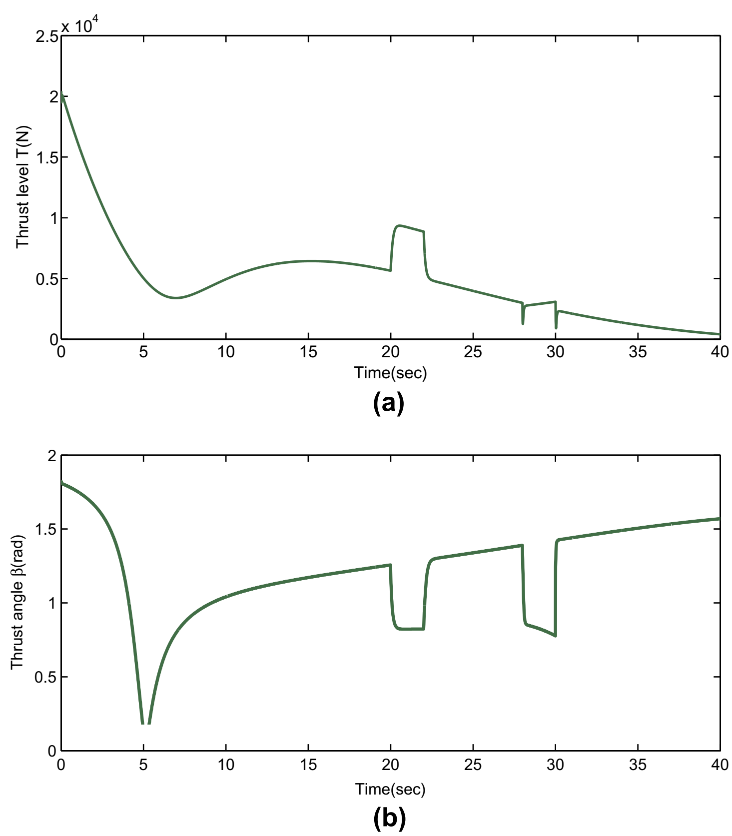

Fig. 9. Response curves of the thrust level and thrust angle of Mars landing model in case 2. (a) T, (b) β.

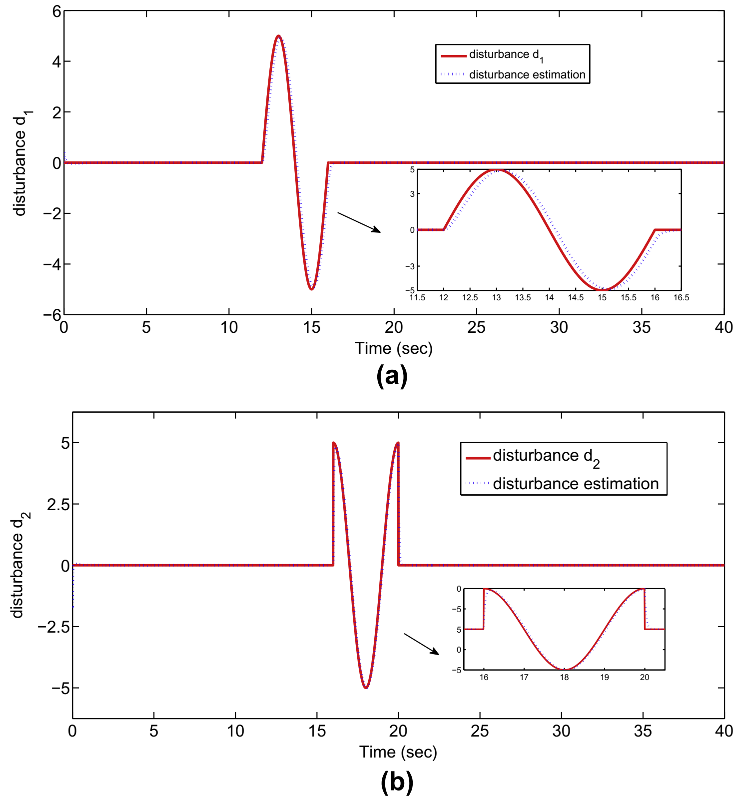

Fig. 10. Response curves of disturbance estimations of Mars landing model in Case 3. (a) $\hat{d}_1$, (b) $\hat{d}_2$.

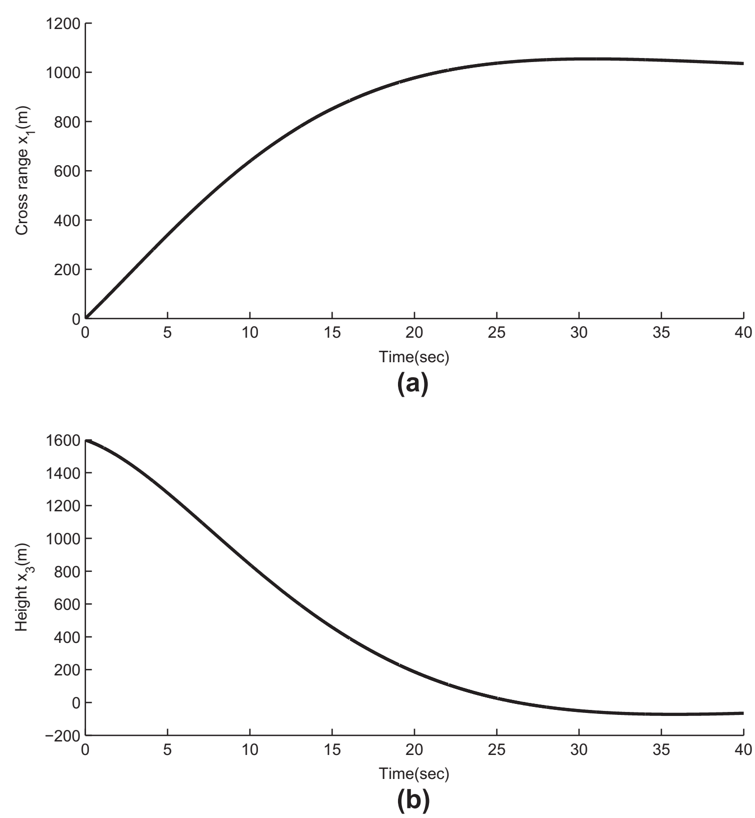

Fig. 11. Response curves of cross range x_1 and height x_3 of Mars landing model in Case 3. (a) x_1, (b) x_3.

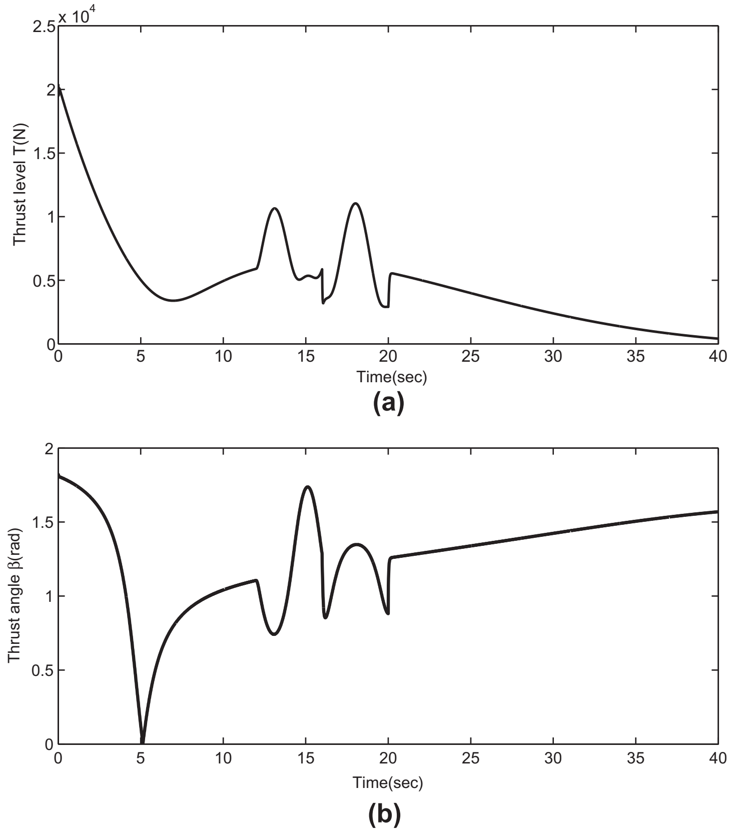

Fig. 12. Response curves of the thrust level and thrust angle of Mars landing model in case 3. (a) T, (b) β.

stability analysis of this controller is omitted here. The simulation results based on the linear controller are illustrated in Figs. 13 and 14. From the figures, we can obtain that it takes much more time for the linear controller to achieve the desire position than our method.

In this paper, we compare our proposed method with the linear controller, the aim is to verify that comprehensive performance(consideration of the convergence of states and energy conservation) of our method is superior to that of the linear control method. Figs. 15 and 16 show the performance index of our method and linear control method. Form the two figures below, we can find that our method is superior to the linear control method in the aspect of considering the convergence of states and energy conservation. In other words, a higher level of thrust T is needed for the linear controller to achieve the same performance as our method.

6. Discussions and conclusion

In this paper, we have applied the θ–D method in the optimal control design with descent model absence of disturbance. However, there are some limitations of the θ–D method respect to the propulsive terminal descent problems. Firstly, because θ–D method is only available for the case of a quadratic cost function, the form of performance index is limited. On the other hand, the constrained optimal control problem cannot be dealt with by θ–D method directly (Xin and Balakrishnan, 2005).

To solve these problems, there are some solutions in existing literatures (de Oliveira and Biegler, 1994; Fletcher, 1987; Fruhwirth and Abdennadher, 2003; Liu and Li, 2013). For example, an improved θ–D technique named the extended θ–D method has been proposed (Liu and Li, 2013), where extended θ–D method is developed for the optimal control problems characterized by a quadratic cost function with a cross term. One can adopt the extended θ–D method if necessary. In practical applications, when the constrained optimal control problem is considered, one can apply the soft constraint method in the controller design by regulating parameters for simulations and practical applications (de Oliveira and Biegler, 1994; Fletcher, 1987; Fruhwirth and Abdennadher, 2003).

In conclusion, this paper has presented a trajectory optimization scheme for powered-descent phase of Mars landing with considerations of disturbance. θ–D method has been applied to design a suboptimal control law with descent model absence of disturbance while the disturbance has been estimated by disturbance observer. Meanwhile, semi-global stability analysis of the composite controller consisting of the nonlinear suboptimal controller and the nonlinear disturbance observer has been given. Finally,

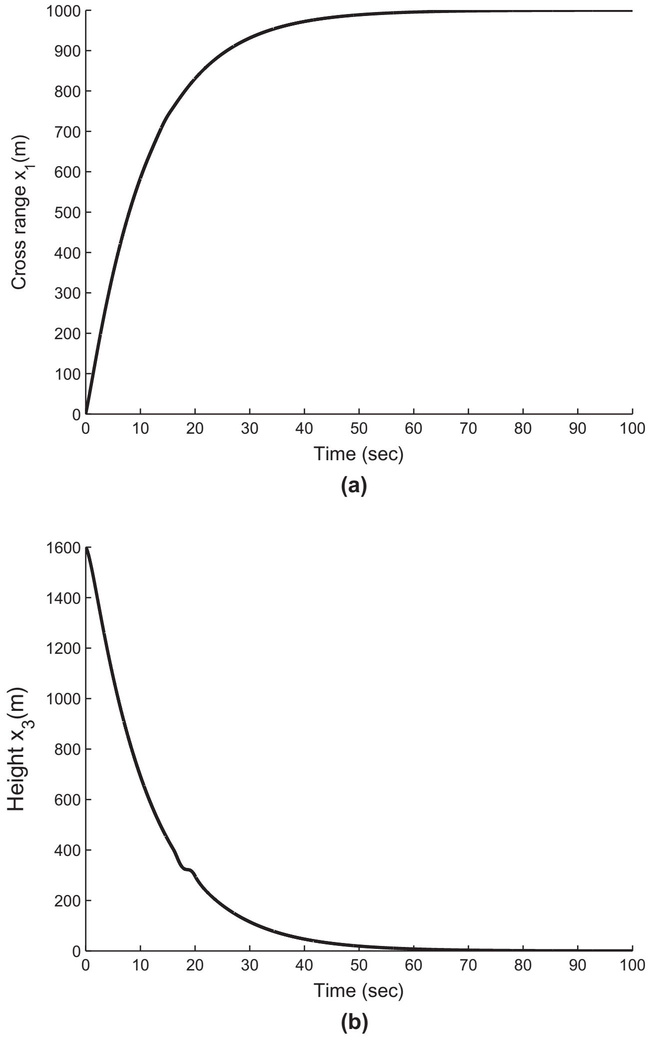

Fig. 13. Response curves of x_1 and x_3 of Mars landing model under linear controller in Case 3. (a) x_1, (b) x_3.

an application including relevant simulations on a Mars landing mission has been demonstrated, which shows the effectiveness and robustness of proposed control scheme. Moreover, extending the model from 2-DOF to multi-DOF, comparing with other advanced control methods and searching for the results of the controller in a Monte Carlo sense will be our next work.

Appendix A.

Proof. In order to prove Theorem 1, here Lemma 4 is mainly applied to the following system:

$$\dot{x} = Ax - BR^{-1}B^T\sum_{i=0}^{\infty}\hat{T}_i x - B_d e_d, \tag{A.1}$$

$$\dot{e}_d = -LB_d e_d - \dot{d}, \tag{A.2}$$

where $e_d = \hat{d} - d$ is the estimation error of the disturbance. As a result, the three conditions in Lemma 4 are needed to be satisfied for system (A.1) and (A.2).

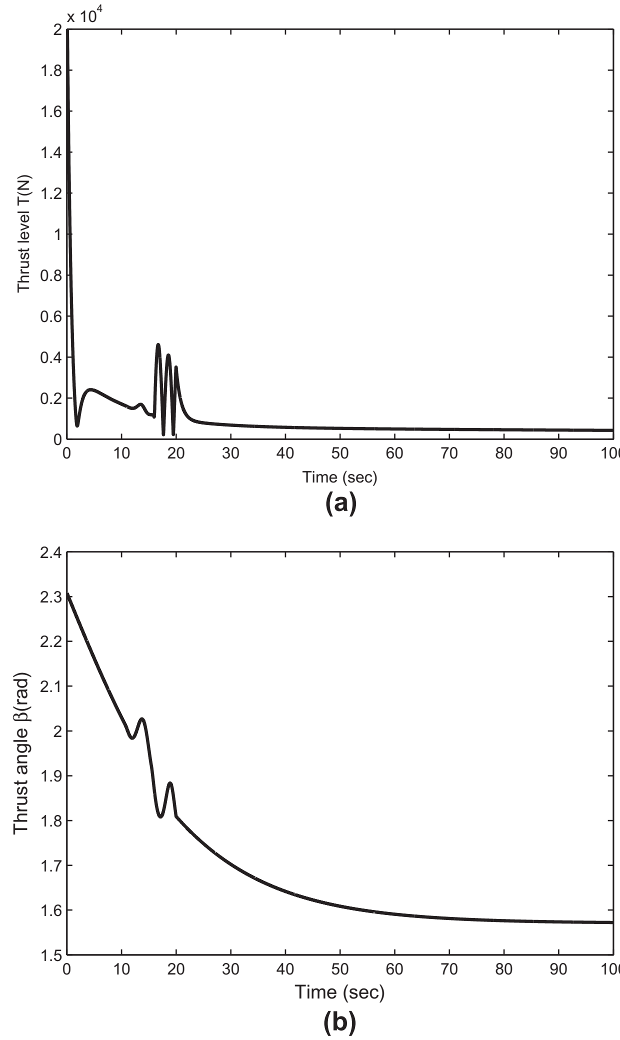

Fig. 14. Response curves of the thrust level and thrust angle of Mars landing model under linear controller in Case 3. (a) u_0, (b) β.

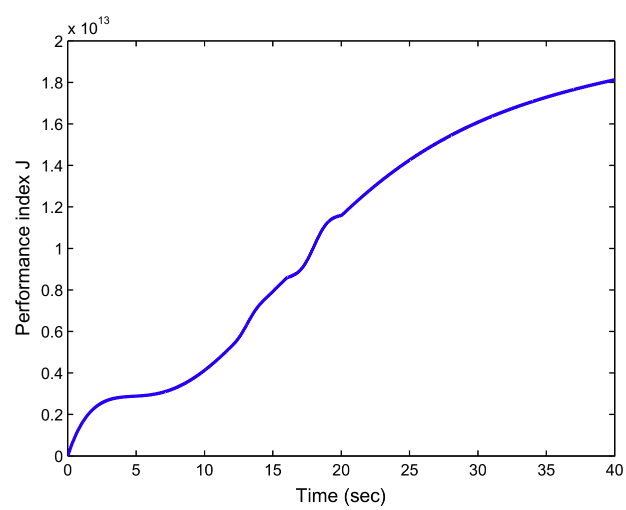

Fig. 15. The performance index of composite controller consisting of the nonlinear suboptimal controller and the disturbance feedforward compensation.

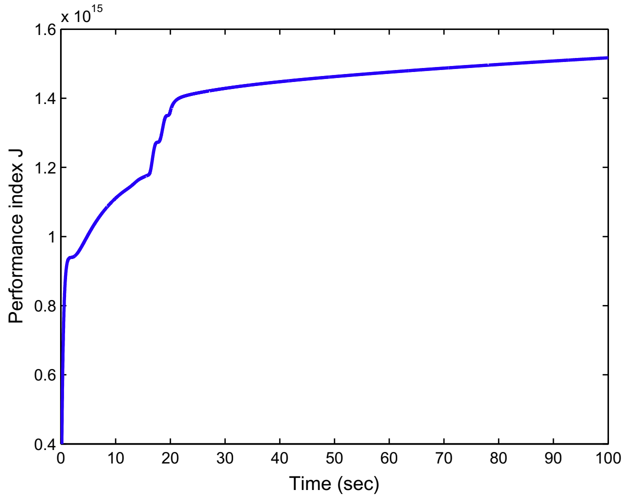

Fig. 16. The performance index of linear controller.

First, for condition (i) in Lemma 4, according to the results in Xin and Balakrishnan (2005), it can be obtained that system (A.1) with $e_d = 0$ is semi-globally asymptotically stable. Thus, condition (i) is satisfied.

Secondly, for condition (ii) in Lemma 4, we prove that system (A.1) is input-to-state stable w.r.t. e_d. Choose a Lyapunov candidate function

$$V(x) = \frac{1}{2} x^T \sum_{i=0}^{\infty} \hat{T}_i x. \tag{A.3}$$

In Lemma 1, it has been proved that $\sum_{i=0}^{\infty} \hat{T}_i$ is pointwise convergent and positive definite. Thus $V(x) > 0$ for $x \neq 0$, and it can be deduced that

$$\lambda_{min} x^T x \leqslant V(x) \leqslant \lambda_{max} x^T x, \tag{A.4}$$

where $\lambda_{min} > 0$, $\lambda_{max} > 0$ are the smallest and largest eigenvalues of $\sum_{i=0}^{\infty} \hat{T}_i$ respectively.

Now,

$$\frac{\partial V(x)}{\partial t} = \left[\frac{\partial V(x)}{\partial x}\right] \dot{x} = \left[\frac{\partial V(x)}{\partial x}\right][Ax + Bu + B_d d] = \left[x^T \sum_{i=0}^{\infty} \hat{T}_i + \frac{1}{2} x^T \sum_{i=0}^{\infty} \frac{\partial \hat{T}_i}{\partial x} x\right][Ax + Bu + B_d d]. \tag{A.5}$$

Since $\sum_{i=0}^{\infty} \hat{T}_i x$ satisfies the HJB equation, one obtains

$$\left[\sum_{i=0}^{\infty} \hat{T}_i x\right]^T [Ax + Bu + B_d d] + \frac{1}{2} u^T R u + \frac{1}{2} x^T \left[Q + \sum_{i=1}^{\infty} D_i \theta^i\right] x = 0.$$

The above equation can be rearranged as follows

$$x^T \sum_{i=0}^{\infty} \hat{T}_i [Ax + Bu + B_d d] = -\frac{1}{2} u^T R u - \frac{1}{2} x^T \left[Q + \sum_{i=1}^{\infty} D_i \theta^i\right] x. \tag{A.6}$$

Since $u = -R^{-1}\left[B^T \sum_{i=0}^{\infty} T_i \theta^i\right] x - C_d \hat{d} = -R^{-1}\left[B^T \sum_{i=0}^{\infty} \hat{T}_i\right] x - C_d \hat{d}$, by substituting the expression of u and (A.6) into (A.5), we have

$$\begin{aligned}\frac{\partial V(x)}{\partial t} = & -\frac{1}{2}\left[B^T \sum_{i=0}^{\infty} \hat{T}_i x - RC_d \hat{d}\right]^T R^{-1} \left[B^T \sum_{i=0}^{\infty} \hat{T}_i x - RC_d \hat{d}\right] \\ & -\frac{1}{2} x^T \left[Q + \sum_{i=1}^{\infty} D_i \theta^i\right] x \\ & + x^T \left[\frac{1}{2} \sum_{i=0}^{\infty} \frac{\partial \hat{T}_i}{\partial x} x \left[A - BR^{-1}\left[B^T \sum_{i=0}^{\infty} \hat{T}_i\right]\right]\right] x \\ & - x^T \left[\frac{1}{2} \sum_{i=0}^{\infty} \frac{\partial \hat{T}_i}{\partial x} x\right] B_d e_d, \end{aligned} \tag{A.7}$$

where $e_d = \hat{d} - d$ is the estimation error of the disturbance.

Since $Q + \sum_{i=1}^{\infty} D_i \theta^i$ is semi-positive definite and R is positive definite, one obtains

$$\left[B^T \sum_{i=0}^{\infty} \hat{T}_i x - RC_d \hat{d}\right]^T R^{-1} \left[B^T \sum_{i=0}^{\infty} \hat{T}_i x - RC_d \hat{d}\right] + x^T \left[Q + \sum_{i=1}^{\infty} D_i \theta^i\right] x > 0.$$

Moreover, for all $\|x\| \geqslant \|B_d\| \|e_d\|$, we have

$$\frac{\partial V(x)}{\partial t} \leqslant -\frac{1}{2} \bar{\lambda} \|x\|^2 + \|x\|^2 \left[\left\|\frac{1}{2} \sum_{i=0}^{\infty} \frac{\partial \hat{T}_i}{\partial x} x\right\| \left(\left\|A - BR^{-1}\left[B^T \sum_{i=0}^{\infty} \hat{T}_i\right]\right\| + 1\right)\right], \tag{A.8}$$

where $\bar{\lambda} = \lambda_{min}\left[Q + \sum_{i=1}^{\infty} D_i \theta^i\right] > 0$.

According to the linearity property of Eqs. (13)–(15), $\hat{T}_i$, $i = 1, \ldots, n$ can always be written as $\epsilon_i \overline{T}_i$, where $\overline{T}_i$ is the solution of Eqs. (13)–(15) without ϵ_i, and

$$\frac{\partial \hat{T}_i}{\partial x} = \frac{\epsilon_i \partial \overline{T}_i}{\partial x}.$$

Thus by choosing ϵ_i, $i = 1, \ldots, n$ properly, we can make that

$$\begin{aligned} & \frac{1}{4} \bar{\lambda} - \left\|\frac{1}{2} \sum_{i=0}^{\infty} \frac{\partial \hat{T}_i}{\partial x} x\right\| \left(\left\|A - BR^{-1}\left[B^T \sum_{i=0}^{\infty} \hat{T}_i\right]\right\| + 1\right) \\ & = \frac{1}{4} \bar{\lambda} - \epsilon_i \left(\left\|\frac{1}{2} \sum_{i=0}^{\infty} \frac{\partial \overline{T}_i}{\partial x} x\right\| \left(\left\|A - BR^{-1}\left[B^T \sum_{i=0}^{\infty} \hat{T}_i\right]\right\| + 1\right)\right) > 0. \end{aligned} \tag{A.9}$$

Note that as long as x lies in a compact set with $R(x)$ bounded, one can always choose a set of ϵ_i such that

$$\frac{\partial V(x)}{\partial t} < -\frac{1}{4} \bar{\lambda} \|x\|^2, \quad \forall \|x\| \geqslant \|B_d\| \|e_d\|. \tag{A.10}$$

Based on Eqs. (A.4) and (A.10), by applying Lemma 2, it yields that system (A.1) is input-to-state stable (ISS) w.r.t. e_d.

Thirdly, for condition (iii), we apply Lemma 2 to prove that system (A.2) is input-to-state stable w.r.t. $\dot{d}$. Here we choose a Lyapunov candidate function

$$\tilde{V} = \frac{1}{2} e_d^T e_d. \tag{A.11}$$

Obviously, it can be derived that the inequality (23) in Lemma 2 is satisfied for system (A.2).

Then we have

$$\begin{aligned} \frac{\partial \tilde{V}}{\partial t} &= e_d^T \dot{e}_d = \frac{1}{2} e_d^T (-LB_d - B_d^T L^T) e_d - e_d^T \dot{d} \\ &\leqslant \frac{1}{2} \tilde{\lambda} \|e_d\|^2 + \|\dot{d}\| \, \|e_d\|, \end{aligned} \tag{A.12}$$

where $\tilde{\lambda}$ is the largest eigenvalue of $-LB_d - B_d^T L^T$, where $\tilde{\lambda} < 0$ as the observer gain matrix L is chosen such that $-LB_d$ is a Hurwitz matrix.

From (A.12), it can be deduced that

$$\frac{\partial \tilde{V}}{\partial t} < \frac{1}{4} \tilde{\lambda} \|e_d\|^2 < 0, \quad \text{for} \quad \|e_d\| > \frac{4\|\dot{d}\|}{-\tilde{\lambda}}, \tag{A.13}$$

where the inequality (24) in Lemma 2 is also satisfied for system (A.2). So, according to Lemma 2, system (A.2) is input-to-state stable w.r.t. $\dot{d}$.

Furthermore, due to Assumption 3 and Lemma 3, it yields that the estimation error e_d converges to 0 as t goes to infinity, which implies that the estimate of DOB can track the disturbances asymptotically.

Therefore, it can be verified that all the three conditions in Lemma 4 are satisfied. Then, based on Lemma 4, system (A.1) and (A.2) is semi-globally asymptotically stable, in other word, system (3) is semi-globally asymptotically stable under control law (21). □

References

Afshari, H., Novinzadeh, A., Roshanian, J. An analytical guidance law of planetary landing mission by minimizing the control effort expenditure. J. Mech. Sci. Technol. 23 (12), 3239–3244, 2009.

Afshari, H., Roshanian, J., Novinzadeh, A. Robust nonlinear optimal solution to the lunar landing guidance by using neighboring optimal control. J. Aerosp. Eng. 24, 20–30, 2011.

Blackmore, L., Açikmeşe, B., Scharf, D. Minimum-landing-error powered-descent guidance for Mars landing using convex optimization. J. Guid. Control Dyn. 33 (4), 1161–1171, 2010.

Braun, R., Manning, R. Mars exploration entry, descent and landing challenges. J. Spacecr. Rockets 44 (2), 310–323, 2007.

Chen, W., Ballance, D., Gawthrop, P., O'Reilly, J. A nonlinear disturbance observer for robotic manipulators. IEEE Trans. Ind. Electron. 47 (4), 932–938, 2000.

Chen, W. Disturbance observer based control for nonlinear systems. IEEE Trans. Mechatron. 9 (4), 706–710, 2004.

de Oliveira, N., Biegler, L. Constraint handling and stability properties of model-predictive control. AIChE J. 40 (7), 1138–1155, 1994.

Fahroo, F., Ross, I. Direct trajection optimization by a Chebyshev pseudospectral method. Proc. Am. Control Conf. 6, 3860–3864, 2000.

Fletcher, R. Practical Methods of Optimization, second ed John Wiley & Sons, 1987.

Fruhwirth, T., Abdennadher, S. Essentials of Constraint Programming. Springer-Verlag Berlin and Heidelberg GmbH & Co. K, 2003.

Gitelson, J.I., Bartsev, S.I., Mezhevikin, V.V., Okhonin, V.A. An alternative approach to solar system exploration providing safety of human mission to Mars. Adv. Space Res. 31 (1), 17–24, 2003.

Izzo, D., Weiss, N., Seidl, T. Constant-optic-flow lunar landing: optimality and guidance. J. Guid. Control Dyn. 34 (5), 1383–1395, 2011.

Khalil, H.K. Nonlinear Systems, third ed Prentice-Hall, Englewood Cliffs, NJ, 2002.

Korzun, A., Dubos, G., Iwata, C., Stahl, B. A concept for the entry, descent, and landing of high-mass payloads at Mars. Acta Astronaut. 66 (7), 1146–1159, 2010.

Li, S., Peng, Y.M., Lu, Y.P., Zhang, L., Liu, Y.F. MCAV/IMU integrated navigation for the powered descent phase of Mars EDL. Adv. Space Res. 46 (5), 557–570, 2010.

Li, S., Peng, Y.M. Mars entry trajectory optimization using DOC and DCNLP. Adv. Space Res. 47 (3), 440–452, 2011.

Li, S., Yang, J., Chen, W., Chen, X. Generalized extended state observer based control for systems with mismatched uncertainties. IEEE Trans. Ind. Electron. 59 (12), 4792–4802, 2012.

Li, S., Yang, J., Chen, W., Chen, X. Disturbance Observer based Control: Methods and Applications. CRC Press, 2013.

Liu, R., Li, S. Suboptimal integral sliding mode design for overhead crane systems. ICIC Express Lett. Part B: Appl. 3 (4), 759–768, 2012.

Liu, R., Li, S. Suboptimal integral sliding mode controller design for a class of affine systems. J. Optim. Theory Appl., http://dx.doi.org/10.1007/s10957-013-0312-x, 2013.

Lukes, D. Optimal regulation of non-linear dynamical systems. SIAM J. Control Optim. 7 (1), 75–100, 1969.

Park, B., Ahn, J., Tahk, M. Two-dimensional trajectory optimization for soft lunar landing considering a landing site. Int. J. Aeronaut. Space Sci. 12 (3), 288–295, 2011.

Sostaric, R. Powered descent trajectory guidance and some considerations for human lunar landing. Adv. Astronaut. Sci. 128, 349–366, 2007.

Steltzner, A.D., Burkhart, P.D., Chen, A., Comeaux, K.A., Guernsey, C.S., Kipp, D.M., Lorenzoni, L.V., Mendeck, G.F., Powell, R.W., Rivellini, T.P., Martin, A., Sell, S.W., Way, R.P. Mars science laboratory entry, descent, and landing system overview, in: International Planetary Probe Workshop, Barcelona, 2010.

Stryk, O., Bulibsch, R. Direct and indirect methods for trajectory optimization. Ann. Oper. Res. 37 (1), 357–373, 1992.

Topcu, U., Casoliva, J., Mease, K. Minimum-fuel powered descent for Mars pinpoint landing. J. Spacecr. Rockets 44 (2), 324–331, 2007.

Wernli, A., Cook, G. Suboptimal control for the nonlinear quadratic regulator problem. Automatica 11 (1), 75–84, 1975.

Xin, M., Balakrishnan, S. New method for suboptimal control of a class of non-linear systems. Optim. Control Appl. Methods 26 (2), 55–83, 2005.

Xin, M., Balakrishnan, S., Pernicka, H. Position and attitude control of deep-space spacecraft formation flying via virtual structure and θ–D technique. J. Dyn. Syst. Meas. Contr. 129 (5), 689–698, 2007.

Xin, M., Balakrishnan, S. Nonlinear H_∞ missile longitudinal autopilot design with θ–D method. IEEE Trans. Aerosp. Electron. Syst. 44 (1), 41–56, 2008.

Yang, J., Zolotas, A., Chen, W., Michail, K., Li, S. Robust control of nonlinear MAGLEV suspension system with mismatched uncertainties via DOBC approach. ISA Trans. 50 (3), 389–396, 2011.

Yang, J., Li, S., Yu, X. Sliding-mode control for systems with mismatched uncertainties via a disturbance observer. IEEE Trans. Ind. Electron. 60 (1), 160–169, 2013.